Inhibition of HIPK2 protects stress-induced pathological cardiac remodeling

Qiulian Zhou,[a,b] Danni Meng,[a,b] Feng Li,[c] Xiao Zhang,[a,b] Li Liu,[a,b] Yujiao Zhu,[a,b] Shuqin Liu,[a,b] Minjun Xu,[a,b] Jiali Deng,[a,b] Zhiyong Lei,[d,e] Joost P.G. Sluijter,[d,f] and Junjie Xiao [a,b]*

[a]Institute of Geriatrics (Shanghai University), Affiliated Nantong Hospital of Shanghai University (The Sixth People's Hospital of Nantong), School of Medicine, Shanghai University, Nantong 226011, China
[b]Cardiac Regeneration and Ageing Lab, Institute of Cardiovascular Sciences, Shanghai Engineering Research Center of Organ Repair, School of Life Science, Shanghai University, Shanghai 200444, China
[c]Research Center for Translational Medicine at East Hospital, Tongji University School of Life Science and Technology, Shanghai, 200092, China
[d]Department of Cardiology, Laboratory of Experimental Cardiology, University Medical Center Utrecht, Utrecht 3508GA, The Netherlands
[e]Central Diagnosis Laboratory Research, Division lab, University Medical Center Utrecht, Utrecht 3508GA, The Netherlands
[f]UMC Utrecht Regenerative Medicine Center, University Medical Center, Utrecht University, Utrecht 3508GA, The Netherlands

Summary

Background Homeodomain-Interacting Protein Kinase 2 (HIPK2) has been reported to maintain basal cardiac function, however, its role in pathological cardiac remodeling remains unclear.

Methods HIPK2 inhibitors (tBID and PKI1H) treated mice and two lines of HIPK2$^{-/-}$ mice were subjected to transverse aortic constriction (TAC). HIPK2 knockdown were performed in neonatal rat cardiomyocytes (NRCMs), neonatal rat cardiac fibroblasts (NRCFs), and human embryonic stem cell-derived cardiomyocytes (hESC-CMs). Microarray analysis was used to screen HIPK2 targets. Overexpression of early growth response 3 (EGR3) and C-type lectin receptor 4D (CLEC4D) were performed in NRCMs, while an activator of Smad3 was used in NRCFs, to rescue the effects of HIPK2 knockdown. Finally, the effects of EGR3 and CLEC4D knockdown by AAV9 in TAC were determined.

Findings HIPK2 was elevated in TAC mice model, as well as cardiomyocyte hypertrophy and NRCFs fibrosis model. Pharmacological and genetic inhibition of HIPK2 improved cardiac function and suppressed cardiac hypertrophy and fibrosis induced by TAC. *In vitro*, HIPK2 inhibition prevented cardiomyocyte hypertrophic growth and NRCFs proliferation and differentiation. At the mechanistic level, we identified EGR3 and CLEC4D as new targets of HIPK2, which were regulated by ERK1/2-CREB and mediated the protective function of HIPK2 inhibition in cardiomyocytes. Meanwhile, inhibition of phosphorylation of Smad3 was responsible for the suppression of cardiac fibroblasts proliferation and differentiation by HIPK2 inhibition. Finally, we found that inhibition of EGR3 or CLEC4D protected against TAC.

Interpretation HIPK2 inhibition protects against pathological cardiac remodeling by reducing EGR3 and CLEC4D with ERK1/2-CREB inhibition in cardiomyocytes, and by suppressing the phosphorylation of Smad3 in cardiac fibroblasts.

---

*Corresponding author at: Cardiac Regeneration and Ageing Lab, Institute of Cardiovascular Sciences, Shanghai Engineering Research Center of Organ Repair, School of Life Science, Shanghai University, 381 Nan Chen Road, Shanghai 200444, China.
   E-mail address: junjiexiao@shu.edu.cn (J. Xiao).

Research in context

Evidence before this study

Homeodomain interacting protein kinase 2 (HIPK2) maintains basal cardiac function by mitogen-activated protein kinase (ERK1/2). The authors previous reported that HIPK2 inhibition could protect myocardial infarction. However, the functional role of HIPK2 in stress-induced pathological cardiac remodeling remains unknown.

Added value of this study

1. HIPK2 inhibition is sufficient to reduce cardiac remodeling and improve heart failure by a dual cellular mechanism including both cardiomyocytes and cardiac fibroblasts.
2. CLEC4D and EGR3 are two downstream targets of HIPK2, mediating its effects in cardiomyocytes hypertrophy.
3. Inhibition of phosphorylation of Smad3 is responsible for the suppression of cardiac fibroblasts proliferation and differentiation by HIPK2 inhibition.
4. Knock-down of EGR3 or CLEC4D protects against TAC induced cardiac remodeling and heart failure.

Implications of all the available evidence

Our findings indicate that inhibition of HIPK2, EGR3 or CLEC4D represent potential novel therapeutic intervention for stress-induced pathological cardiac remodeling.

Introduction

Heart failure is the final stage of most cardiovascular diseases and one of the leading causes of death worldwide.[1] Pathological myocardial remodeling is an early sign and a risk factor of heart failure, which may be caused by multiple stresses including hypertension and myocardial infarction.[2−5] However, the regulatory mechanisms of pathological cardiac remodeling and heart failure remain to be fully elucidated.[2−5] On the other hand, although increasingly advanced medical therapies can improve the symptoms of heart failure, it is still unable to prevent further development or reverse pathological progression.[2−5] There is an urgent need of developing effective treatments of heart failure.[2−5]

Homeodomain-interacting-protein-kinase 2 (HIPK2) with a conserved protein kinase domain interacting with homologous proteins, belongs to a nuclear serine/threonine kinase family composed of four proteins (HIPK 1, 2, 3 and 4) and is involved in the regulation of a variety of biological processes including signal transduction, DNA damage response, cell proliferation, embryonic development and apoptosis.[6−8] Previous studies have shown that HIPK2 participates in differentiation and development such as neurogenesis, myogenesis, angiogenesis, adipogenesis and hematopoiesis.[9−11] Myocyte enhancer factor 2 (MEF2), p53, transforming growth factor beta (TGF-β)/ small mothers against decapentaplegic (Smad) 3, Wnt/β-catenin, nuclear factor kappa B (NF-κB) have been identified as classic down-stream targets of HIPK2.[10,12−15] A recent study showed that HIPK2 maintained basal cardiac function by mitogen-activated protein kinase (ERK1/2).[16] Our previous work showed miR-222, a cardiac protective factor, targets HIPK2 to execute its functions.[17] More recently, we reported that HIPK2 inhibition could protect myocardial infarction.[18] However, the exact role of HIPK2 in pathological cardiac remodeling and heart failure is not known.

In the present study, we show that HIPK2 expression is elevated in myocardium from transverse aortic constriction (TAC) mice and human left ventricle of heart failure patients. Treatment by HIPK2 inhibitors, 4,5,6,7-tetrabromo-2- (1H-imidazol- 2-yl)isoindoline-1,3-dione (tBID)[19] and protein kinase inhibitors 1 hydrochloride (PKI1H)[20] reverses impaired cardiac function induced by TAC, a finding recapitulated in HIPK2$^{-/-}$ mice. Moreover, HIPK2 inhibition prevents cardiomyocyte hypertrophy in neonatal rat cardiomyocytes (NRCMs) and human embryonic stem cell-derived cardiomyocytes (hESC-CMs), and suppresses proliferation and differentiation of neonatal rat cardiac fibroblasts (NRCFs). At the mechanistic level, we identify early growth response 3 (EGR3) and C-type lectin receptor 4D (CLEC4D) as targets of HIPK2 in cardiomyocytes and they are regulated by ERK1/2-CREB. Additionally, phosphorylation of Smad3 is involved in HIPK2 suppression-mediated cardiac protection through fibroblasts. Finally, we report that inhibition of EGR3 or CLEC4D protects against TAC induced cardiac dysfunction. Taken together, our study uncovered distinct protective roles of HIPK2 inhibition in cardiomyocytes and fibroblasts, respectively, indicating that inhibition of HIPK2 might be a therapeutic intervention in ameliorating pathological cardiac remodeling and heart failure.

Methods

Ethics statement, animals and treatments

Male C57BL/6 wild-type (WT) mice aged 8-week-old were obtained from Cavens Laboratory Animal Ltd. (Changzhou, China). Two founders of C57BL/6 HIPK2$^{-/-}$ mice were generated in Beijing Viewsolid Bioteh Co. Ltd (Beijing, China) by embryo injection of CRISPRs targeting the second exon (guide RNA sequences: AAGTTC-CAACTGGGACATGACTGGGT) of the mouse *HIPK2* gene. One founder (line 1) with frameshift mutations (56bp deletion: TGGGTACGGCTCCCACAGCA AAGTG-TACAGCCAGAGCAAGAACATACCACCTTCTC) and another founder (line 2) with frameshift mutations (40bp deletion: AAAGTGTACAGCCAGAGC AAGAACATAC-CACCTTCTCAGC) were identified and crossed with

C57BL/6 WT mice for colony expansion and subsequent experiments. Tail biopsies of HIPK2$^{-/-}$ mice were analyzed by genomic PCR (forward primer 5'- TTCA-GAGTGGAAG AACAATC -3' and reverse primer 5'-TTGGTAGG TGTCAAGGAG -3'). All mice were maintained on a 12 h light/dark cycle at 25 °C and provided free access to commercial rodent chow and tap water. Tissues were isolated and snap-frozen for future analysis or put into 4% paraformaldehyde buffer (PFA) immediately for histological study. These experiments were conducted in accordance with guidelines of laboratory animals for biomedical research published by National Institutes of Health (No. 85−23, revised 1996) and approved by the ethical committees of Shanghai University (Approval number: 2018011).

At the end of the experiments, mice were sacrificed via intraperitoneal sodium pentobarbital (60 mg/kg) and cardiac tissues were analyzed.

Transverse aortic constriction model

Mice maintained body temperature at 37 °C on a heating pad were anesthetized with 2% isoflurane and intubated with a rodent ventilator. Left ventricular pressure overload was produced in mice by transverse aortic constriction between the innominate and left common carotid arteries using a blunted needle (27-gauge) positioned parallel to the aorta and a 7/0 silk thread. The incision was closed at last. The sham group was subjected to an identical procedure without aortic constriction.

For HIPK2 inhibitors treatment, mice were oral administration with 200 μg/kg/day tBID (MedChemExpress, USA), 200 μg/kg/day PKI1H (MedChemExpress, USA) or phosphate-buffered saline (PBS) once a day for 4 weeks after operation. All mice were sacrificed after 4 weeks.

Cardiac ischemia-reperfusion injury model

Cardiac I/R injury was induced by ligation of the left anterior descending artery (LAD) for 30 min followed by cardiac reperfusion while sham was created by the same process but without LAD ligation as previously reported.[21] All mice were sacrificed after 3 weeks.

Echocardiography

Fractional shortening (FS), left ventricular (LV) mass, left ventricular internal dimension (LVID) and left ventricular posterior wall (LVPW) were evaluated by Vevo 2100 echocardiography (VisualSonics Inc, Canada) with a 30 MHz central frequency scan head in mice anesthetized with 1.5% isoflurane and measured from M-mode images taken from the parasternal long-axis view at papillary muscle level with at least three measurements for each mouse.

Tissues morphological analysis

Sections of hearts samples with 5 μm thick sections fixed in 4% PFA and embedded in paraffin were stained with Masson's trichrome (KeyGen, China) to detect the degree of collagen deposition, or hematoxylin and eosin (H&E, KeyGen, China) to measure cardiomyocytes cross-sectional areas, or CD31 (1:100, Cell Signaling Technology, USA) immunohistochemical staining to measure myocardial capillary density. Images of the left ventricular area of each section were obtained by microscope (Nikon, Japan). Frozen sections of hearts in O.C.T Compound (optimal cutting temperature compound, Sakura, USA) were cut at 5 μm per section and stained with wheat germ agglutinin (WGA, Sigma, USA) to measure cardiomyocytes cross-sectional areas. Fluorescence images were obtained using a Zeiss confocal microscope (Carl Zeiss, Germany). Image J Software (National Institutes of Health) was used to quantify fibrotic region and measure cardiomyocytes cross-sectional areas in each section. The percentage of fibrosis was measured as fibrosis areas/total left ventricular areas x 100%.

AAV9 construction and administration

Mouse shEGR3 and shCLEC4D were cloned into AAV9 generating plasmid and then packaged into AAV9 virus (Hanbio Co. Ltd, China). The sequences are CCGGAACTCTCTTATTCGAGCTCTT for EGR3 and CTTCCAGTCTAACTGTT ACTT for CLEC4D. AAV9 virus was delivered by tail vein injection at a dose of $3*10^{11}$ TU/mice a week before the surgery, and all mice were sacrificed after 4 weeks after TAC.

Lentivirus construction and administration

The shRNA sequence for HIPK2 was 5'- GTATGATCA-GATTCGGTATAT-3' and cloned into the pLKO.1-TRC cloning vector. The DNA fragments encoding rat HIPK2, EGR3 and CLEC4D was amplified from rat heart genomic complementary DNA (cDNA) and cloned into the FUGW cloning vector. Lentiviral particles were generated and packaged using psPAX2 and PMD2.G. Lentiviruses were diluted in PBS and administered at a dose of 10^7 TU/well in 12-well plates for 48 h.

Whole-genome gene expression

Total RNA from heart of control WT littermates and HIPK2$^{-/-}$ mice (line 1) was extracted and hybridized on Agilent SurePrint G3 Mouse GE V2.0 Microarray (8*60K, Design ID:074809) (OE Biotech's, Shanghai, China). The expression data are available in NCBI Gene Expression Omnibus (GEO, platform ID: GSE169429).

Cell isolation, culture and treatments

Adult mouse cardiomyocytes (MCMs), adult mouse cardiac fibroblasts (MCFs), adult rat cardiac fibroblasts

(RCFs), neonatal rat cardiomyocytes (NRCMs) and neonatal rat cardiac fibroblasts (NRCFs) were isolated from ventricle of adult mice, adult rat or neonatal rat and cultured as previously reported.[22,23] Human cardiomyocyte cell line AC16 cells were cultured as previously reported.[18] For Phenylephrine (PE, TOCRIS, USA) treatment, NRCMs were treated with PE at 100 μM for 48 hours.[24−27] For TGF-β (Peprotech, USA) treatment, NRCFs or RCFs were treated with recombinant human TGF-β1 at 10 ng/ml for 24 hours.[21] For HIPK2 inhibition, cells were treated with HIPK2 inhibitors, tBID or PKI1H, at 1 μM or 74 nM for 48 hours respectively. For ERK1/2 inhibition, NRCMs were treated with PD98059 (S1177, Selleck, USA) at 50 μM for 24 hours. For ERK1/2 activation, NRCMs were treated with Ceramide C6 (SC-3527, Santa Cruz, USA) at 10 μM for 24 hours. For Smad3 activation, cardiac fibroblasts were treated with Alantolactone (HY-N0038, MedChemExpress, USA) at 2 μg/ml for 4 hours. The double-stranded siRNA targeting rat EGR3 and CLEC4D were 5'-CCAAUCCGGAACUCUCUUAUU-3' and 5'-CAACCC AAACGUGGUAUU CUGGAAA-3' respectively. Cells were transfected with siRNA using Lipofectamine2000.

Human embryonic stem cells cell line H9 were cultured on Matrigel (Corning) coated plates and mTeSR medium (Stemcell) supplemented with Y-27632 (10 μM, Selleck) in feeder-free culture conditions. On day 0, differentiation was induced by CHIR99021 (6 μM, Selleck) for 48 hours. The medium was refreshed with addition of Wnt-pathway inhibitor IWP2 (5 μM, Selleck) for 48 hours. The basal medium is RPMI 1640 medium (Life Technologies) supplemented with Albumin (0.5 mg/ml) and ascorbic acid (0.2 mg/ml). Spontaneous beating cells start to appear at day 8, and the beating cells were cultured in RPMI 1640 supplemented with B27 for further maturation. Culture medium was changed every two days. Human embryonic stem cell-derived cardiomyocytes (hESC-CMs) were used after differentiation for 30 days.[28] For hypertrophy model, hESCs-CMs were treated with phenylephrine (PE, Toris) and Isoproterenol (ISO, Sigma).[29] The PE and ISO were added in culture medium at 100 μM for 48 hours, and the plates were covered with aluminium foil during the treatment. For HIPK2 suppression, PKI1H (74 nM) were incubated for 48 hours.

Flow cytometry
Cardiac fibroblasts were fixed with 4% paraformaldehyde (PFA) for 20 min, permeabilized with 0.25% Triton X-100 for 20 min, blocked with 5% bovine serum albumin in PBS-Tween for 1 h, incubated with the primary antibody (α-SMA antibody, 1:500, Sigma, USA) for 1 h and the second antibody (APC-goat anti mouse IgG (H+L), 1:200) for 1 h in dark. The cells were incubated with EdU for 30 min, and then the cells were subjected to 50 μm filter screen and flow detection.

Immunofluorescent staining for EdU, α-SMA, α-actinin, Vimentin, HIPK2 and Hoechst
NRCMs and NRCFs were fixed with 4% PFA for 20 min, permeabilized with 0.2% Triton X-100 for 20 min and blocked with 10% goat serum in PBS-Tween for 1 h. Subsequently, NRCMs were incubated with α-actinin antibody diluted in 10% goat serum and NRCFs were incubated with α-SMA-Cy3 antibody (1:500, Sigma, USA) overnight at 4°C. To detect proliferation, EdU assays were performed using Click-iT Plus EdU Alexa Fluor 488 Imaging Kit (Invitrogen) according to manufacturer's instructions. Cell nuclei were counterstained with Hoechst and the number of EdU-positive nuclei was calculated. Fifteen fields/sample (200 x magnification) were viewed under a confocal microscope (Carl Zeiss, Germany).

Frozen sections of hearts were fixed in 4% paraformaldehyde (PFA) for 20 min, and permeabilized with 0.5% Triton X-100 for 20 min, then blocked with 5% BSA for 1 hour at room temperature. Subsequently, sections of hearts were incubated with HIPK2 Polyclonal antibody (1:200, Proteintech, USA) and mouse monoclonal anti-α-actinin (1:200, Sigma, USA) for cardiomyocytes or mouse monoclonal anti-Vimentin antibody (1:200, Abcam, UK) for fibroblasts overnight at 4°C. Then, sections were incubated for 2 hours at room temperature with the secondary antibody (1:200). And then nucleus were counterstained with Hoechst (1:2000) for 20 min at room temperature. The relative fluorescence intensity of HIPK2 in cardiomyocytes (α-actinin positive) and cardiac fibroblasts (Vimentin positive) were calculated. Twenty fields/sample (40 x magnification) were viewed under a confocal microscope (Olympus, Japan).

RNA isolation and relative quantitative RT-PCR
RNA isolation and relative quantification RT-PCR were performed as described previously.[23] The sequences of primers used for RT-PCR are listed in Supplemental Table S1.

Western blotting
Protein extraction and immunoblotting assays were performed as previously described.[30] All antibodies used in this study were listed in RRID tags.

Statistical analysis
All data were expressed as mean ± SD. Significant differences were assessed either by two-tailed student t-test, one-way ANOVA followed by Bonferroni's post hoc test, or two-way ANOVA followed by Bonferroni's multiple comparisons test. P values less than 0.05 were considered to be statistically different. All analyses were performed using GraphPad Prism 8.0.

RRID tags

| Reagent or resource	Source	Identifier	RRID
Antibodies			
HIPK2	Abcam	ab108543	AB_10860868
HIPK2	Proteintech	55408-1-AP	AB_2881323
β-actin	Bioworld	AP0060	AB_2797445
Collagen1	Bioworld	BS1530	AB_1662101
EGR3	ABclonal	A7669	AB_2769279
CLEC4D	ABclonal	A2697	AB_2764553
CRLF1	ABclonal	A17589	AB_2769048
ADAMTS4	ABclonal	A2525	AB_2764416
FBN1	ABclonal	A16677	AB_2769423
P-Smad3(S423/425)	ABclonal	AP0727	AB_2863813
P-Smad3(T179)	Abcam	ab74062	AB_1524418
Smad3	ABclonal	A19115	AB_2862608
P-ERK1(T202/Y204) + ERK2(T185/Y187)	ABclonal	AP0974	AB_2863871
ERK1/2	ABclonal	A4782	AB_2863347
P-CREB (S133)	Abcam	ab254107	AB_2922394
CREB 1	ABclonal	A0826	AB_2757415
Bax	ABclonal	A12009	AB_2861644
Bcl2	Affinity	AF6139	AB_2835021
Caspase3	ABclonal	A2156	AB_2862975
GAPDH	Bioworld	AP0063	AB_2651132
α-SMA-Cy3	Sigma-Aldrich	C6198	AB_476856
CD31	CST	77699S	AB_2722705
Vimentin	Abcam	ab8978	AB_306907
Cell Lines			
AC16	Millipore	SCC109	CVCL_4U18
H9			CVCL_9773
Chemicals, Peptides, and Recombinant Proteins			
PE (Phenylephrine)	TOCRIS	2838	
Recombinant Human TGF-β1	Peprotech	100-21C	
tBID	MedChemExpress	HY-100464	
PKI1H (Protein kinase inhibitors 1 hydrochloride)	MedChemExpress	HY-U00439A	
PD98059	Selleck	s1177	
Ceramide C6	Santa Cruz	SC-3527	
Alantolactone	MedChemExpress	HY-N0038	
WGA (wheat germ agglutinin)	Sigma	L4895	
Critical Commercial Assays			
Western Blot lysis buffer	KeyGEN	KGP701-100	
TaKaRa BCA Protein Assay Kit	Takara	T9300A	
Masson's trichrome staining Kit	KeyGEN BioTECH	KGMST-8003	
H&E staining Kit	KeyGEN BioTECH	KGA224	
TUNEL FITC Apoptosis Detection Kit	Vazyme	A111-01	
Software and Algorithms			
ImageJ Software	NIH	N/A	
GraphPad Prism 8.0	GraphPad	N/A	
Vevo2100	VisualSonic	N/A	
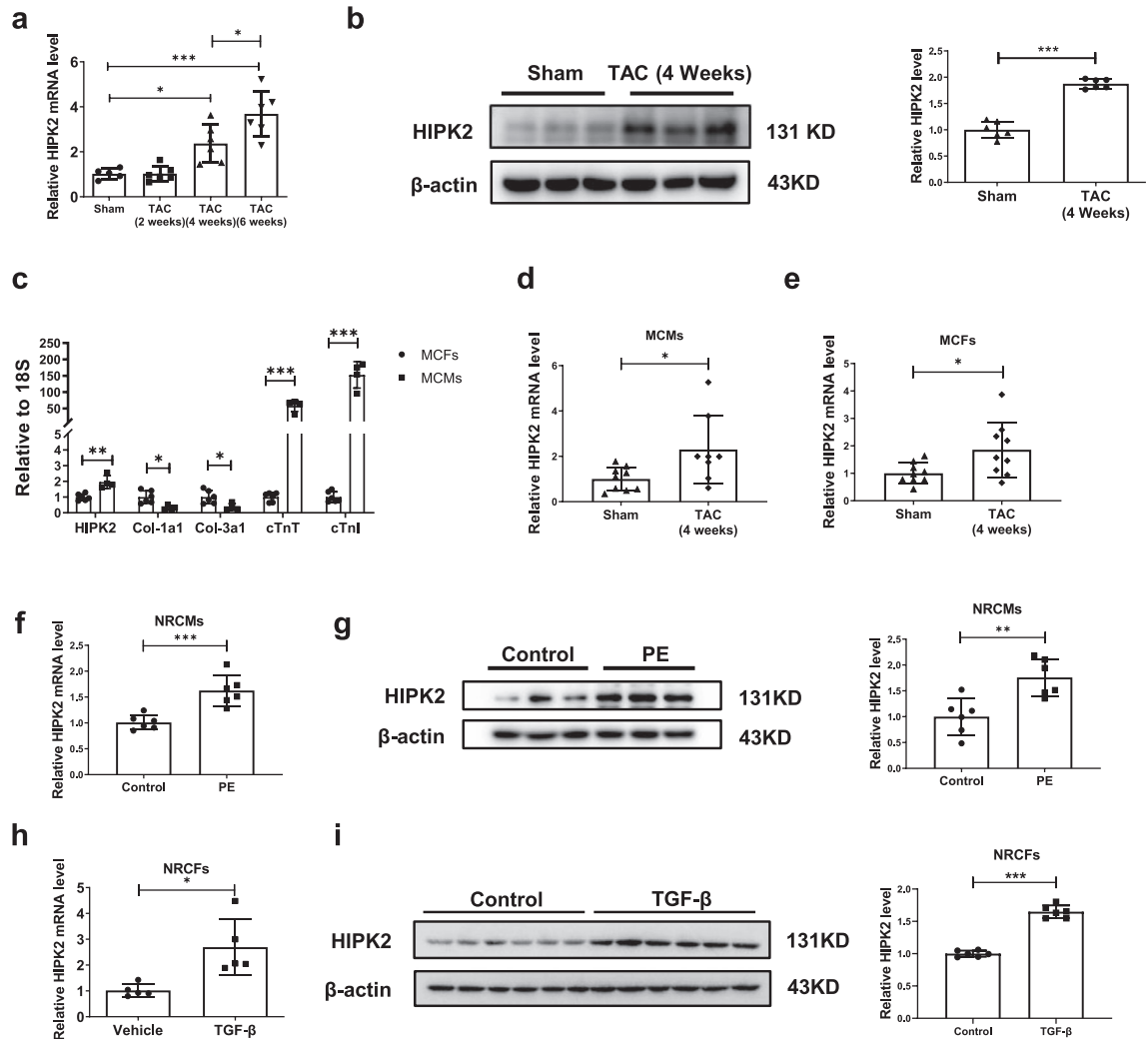
Figure 1. HIPK2 is elevated in pathological cardiac remodeling. (a) Cardiac HIPK2 mRNA levels were increased in male C57BL/6 wild-type (WT) mice subjected to transverse aortic constriction (TAC) compared to sham operation (sham) at 2, 4 or 6 weeks after operation (n=5:6:6:6); (b) Cardiac HIPK2 protein levels were increased in TAC compared to sham at 4 weeks after operation (n=6); (c) HIPK2 was more abundance in MCMs as compared to MCFs; cTnT, cTnI, Col1a1, and Col3a1 were used as markers for MCMs and MCFs (n=6:4); (d) HIPK2 mRNA levels were increased in MCMs of TAC compared to sham mice (n=9:8); (e) HIPK2 mRNA levels were increased in MCFs of TAC compared to sham mice (n=9); (f and g) HIPK2 mRNA levels (n=6) and HIPK2 protein levels (n=6) were increased in NRCMs treated with PE compared to Control; (h and i) HIPK2 mRNA levels (n=5) and HIPK2 protein levels (n=6) were increased in NRCFs treated with TGF-β compared to Control. Significant differences were assessed by one-way ANOVA followed by Bonferroni's post hoc test in a, or two-tailed student t-test in b-i. *: $p<0.05$, **: $p<0.01$, ***: $p<0.001$ versus respective control.

Role of funding source

The Funders do not play any roles in study design, data collection, data analyses, interpretation, or writing of report.

Results

HIPK2 is elevated in pathological cardiac remodeling

To determine the role of HIPK2 in pathological cardiac remodeling, we subjected wild-type mice to TAC.

Cardiac HIPK2 mRNA expression level was significantly increased at 4 weeks after TAC, and was further increased at 6 weeks after TAC (Figure 1a). Consistently, HIPK2 protein level was up-regulated at 4 weeks after TAC (Figure 1b).

To investigate the roles of HIPK2 in cardiomyocytes and cardiac fibroblasts, respectively, we isolated adult mouse cardiomyocytes (MCMs) and adult mouse cardiac fibroblasts (MCFs). We found that HIPK2 mRNA level was lower in MCFs than in MCMs (Figure 1c). Furthermore, we showed that HIPK2 mRNA expression

was elevated in both MCMs and MCFs of TAC mice (Figure 1d-e). Moreover, based on α-actinin and HIPK2, or Vimentin and HIPK2 immunofluorescent staining, we found that HIPK2 was increased in both cardiomyocytes and cardiac fibroblasts of TAC (Supplemental Figure S1). In addition, we found that HIPK2 mRNA and protein expression levels were increased in NRCMs after PE treatment (Figure 1f-g), and up-regulated in NRCFs treated with TGF-β (Figure 1h-i).

Captopril and metoprolol are used to treat heart failure patients in the clinic. We used captopril (10 mg/kg/d) or metoprolol (30 mg/kg/d) in TAC mice and found that captopril or metoprolol decreased HIPK2 mRNA and protein levels in TAC (Supplemental Figure S2). Moreover, we analyzed the expression of HIPK2 from GEO database (GSE161473).[31] We found that HIPK2 was elevated in human left ventricle of heart failure with reduced ejection fraction (HFrEF) patients (Supplemental Figure S3).

Collectively, these data indicate that HIPK2 is elevated in pathological cardiac remodeling.

Inhibition of HIPK2 protects against cardiac dysfunction under stress

As we demonstrated that HIPK2 was elevated in pathological cardiac remodeling, we next asked whether HIPK2 inhibition might be protective for cardiac dysfunction under stress. Two specific distinct HIPK2 inhibitors (tBID and PKI1H) were used[19,20] and we found that both HIPK2 inhibitors increased fractional shortening (FS), and decreased LV mass, LVIDs, and LVPWd in mice subjected to TAC (4 weeks) (Figure 2a). Moreover, inhibition of HIPK2 decreased cardiac fibrosis and cardiomyocyte hypertrophy as evidenced by reduced collagen deposition, cardiomyocyte cross sectional area, heart weight (HW)/body weight (BW), and HW/tibial length (TL) (Figure 2b-c and Supplemental Figure S4a-b). Besides, inhibition of HIPK2 decreased cardiac ANP, BNP, Col1a1, Col3a1, and α-SMA mRNA expression post-TAC, and increased the ratio of α-MHC and β-MHC post-TAC (Figure 2d). Additionally, the expression of Collagen1, the ratio of Bax and Bcl$_2$ (Bax/Bcl$_2$), the ratio of cleaved Caspase3 and Caspase3 (cleaved Caspase3/Caspase3) were markedly decreased by HIPK2 inhibitors in the TAC group (Supplemental Figure S4c). Additionally, inhibition of HIPK2 promoted myocardial capillarity after TAC (Supplemental Figure S5).

To further illustrate the role of HIPK2, we generated HIPK2$^{-/-}$ mice by CRISPR/Cas9 genome-editing technology confirmed HIPK2 depletion in vivo (Supplemental Figure S6a-c). Consistently, HIPK2$^{-/-}$ mice showed significantly improvements in cardiac function after TAC (4 weeks) (Figure 3a-d, Supplemental Figure S7 and S8). To confirm the protective effects of HIPK2 knockout in TAC, the other line of HIPK2$^{-/-}$ mice

(line-2) was also tested. Similarly, HIPK2$^{-/-}$ line-2 mice attenuated cardiac dysfunction after TAC (Supplemental Figure S9). Considering the similar protective effects of these two lines of HIPK2$^{-/-}$ mice, we mostly use line-1 to explore the role of HIPK2 deficiency in the heart.

Taken together, these findings suggest that inhibition of HIPK2 protects the heart from pathological cardiac hypertrophy and fibrosis in vivo.

Inhibition of HIPK2 prevents cardiomyocyte hypertrophy, fibroblast proliferation and differentiation

Given the up-regulation of HIPK2 in both MCMs and MCFs from the TAC mice, we hypothesized that HIPK2 might function in both cell types. To test this hypothesis, we examined the effect of HIPK2 inhibition on cardiomyocyte hypertrophy and cardiac fibroblast proliferation and differentiation.

Although HIPK2 overexpression showed no effect on cell size in NRCMs treated with PE (Supplemental Figure S10a-b), knockdown of HIPK2 with lentivirus (Lenti-shHIPK2) reduced cell size and expression levels of ANP and BNP in NRCMs treated with PE (Figure 4a-c, Supplemental Figure S10c-d). Consistently, HIPK2 inhibitors, tBID and PKI1H, showed the same effect as Lenti-shHIPK2 in NRCMs treated with PE (Figure 4d-f, and Supplemental Figure S11). To further confirm the human relevance of our findings, we tested the effect of HIPK2 inhibition in human embryonic stem cell-derived cardiomyocytes (hESC-CMs). We found that HIPK2 inhibition by PKI1H could attenuate cardiomyocytes hypertrophy induced by PE and ISO in hESC-CMs (Supplemental Figure S12).

The increased proliferation and differentiation of cardiac fibroblasts into myofibroblasts is a key step in the development of cardiac fibrosis. Although HIPK2 overexpression showed no effect on NRCFs proliferation and differentiation into myofibroblasts (Supplemental Figure S13a-c), we found that Lenti-shHIPK2 decreased proliferation and transformation of fibroblasts into myofibroblasts in NRCFs incubated with TGF-β (Figure 5a-c, Supplemental Figure S13d-e). Consistently, HIPK2 inhibitors, tBID and PKI1H, showed the similar inhibitory effect as Lenti-shHIPK2 in NRCFs and RCFs with TGF-β treatment (Figure 5d-g, and Supplemental Figure S14).

Taken together, our data demonstrate that inhibition of HIPK2 prevents cardiomyocyte hypertrophy, and cardiac fibroblast proliferation and differentiation.

CLEC4D and EGR3 are responsible for the protective effects of HIPK2 inhibition in cardiac hypertrophy

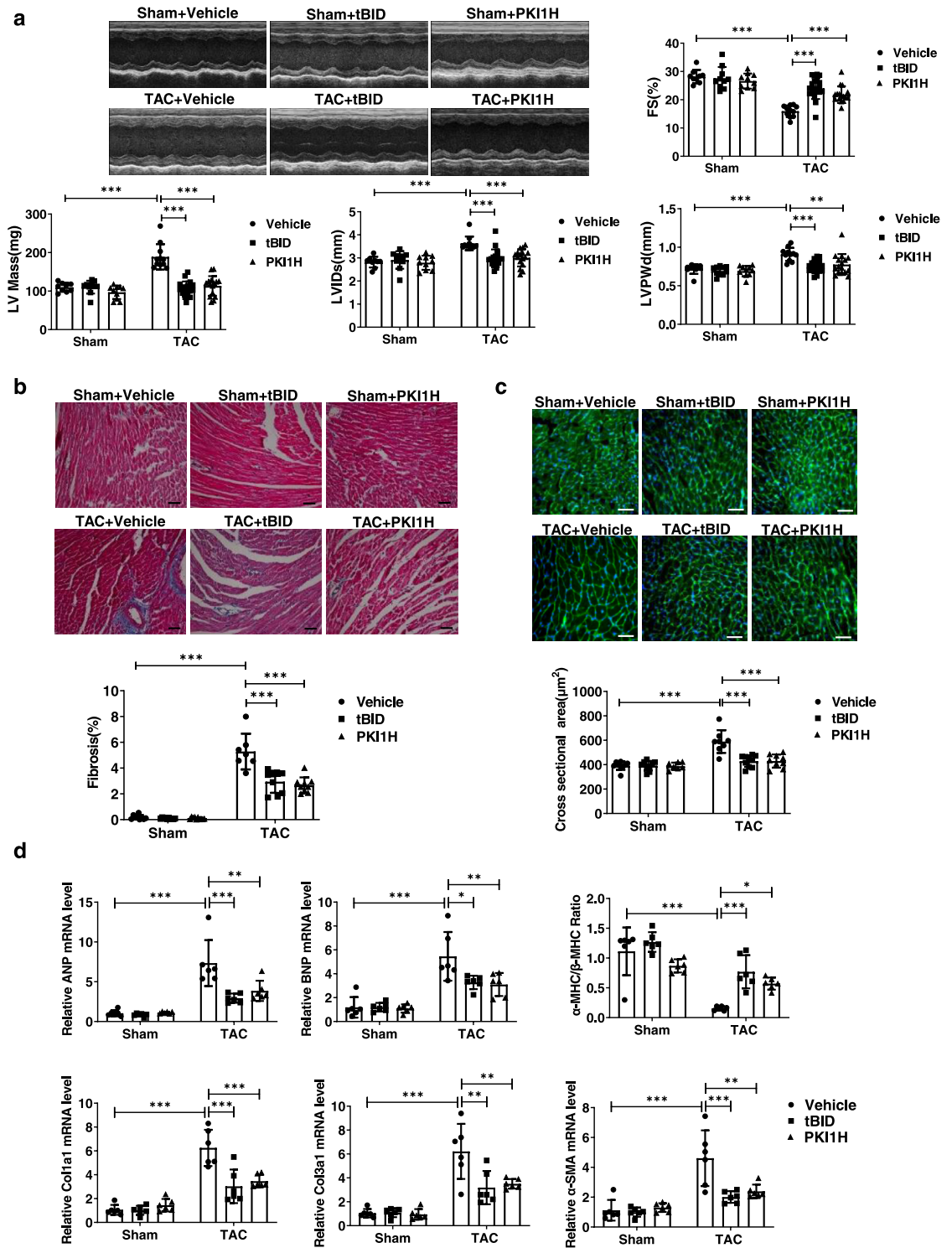To identify downstream targets of HIPK2 in the heart, we conducted an unbiased screening using the

Figure 2. HIPK2 inhibition protects against cardiac dysfunction after TAC. (a) tBID and PKI1H increased fractional shortening (FS) post-TAC, and reduced left ventricular (LV) mass, left ventricular systolic internal dimension (LVIDs) and left ventricular diastolic posterior wall (LVPWd) post-TAC (n=9:10:10:11:18:16); (b) tBID and PKI1H reduced cardiac fibrosis post-TAC (n=9:10:10:7:9:9); (c) tBID and PKI1H reduced cross sectional area of cardiomyocytes post-TAC (n=9:9:7:8:10:9); (d) tBID and PKI1H decreased cardiac ANP, BNP, Col1a1, Col3a1, and α-SMA mRNA expression post-TAC, and increased ratio of α-MHC and β-MHC post-TAC (n=6). Scale bar: 50 μm in b and c. Significant differences were assessed by two-way ANOVA followed by Bonferroni's multiple comparisons test. *: $p < 0.05$, **: $p < 0.01$, ***: $p < 0.001$ versus respective control.
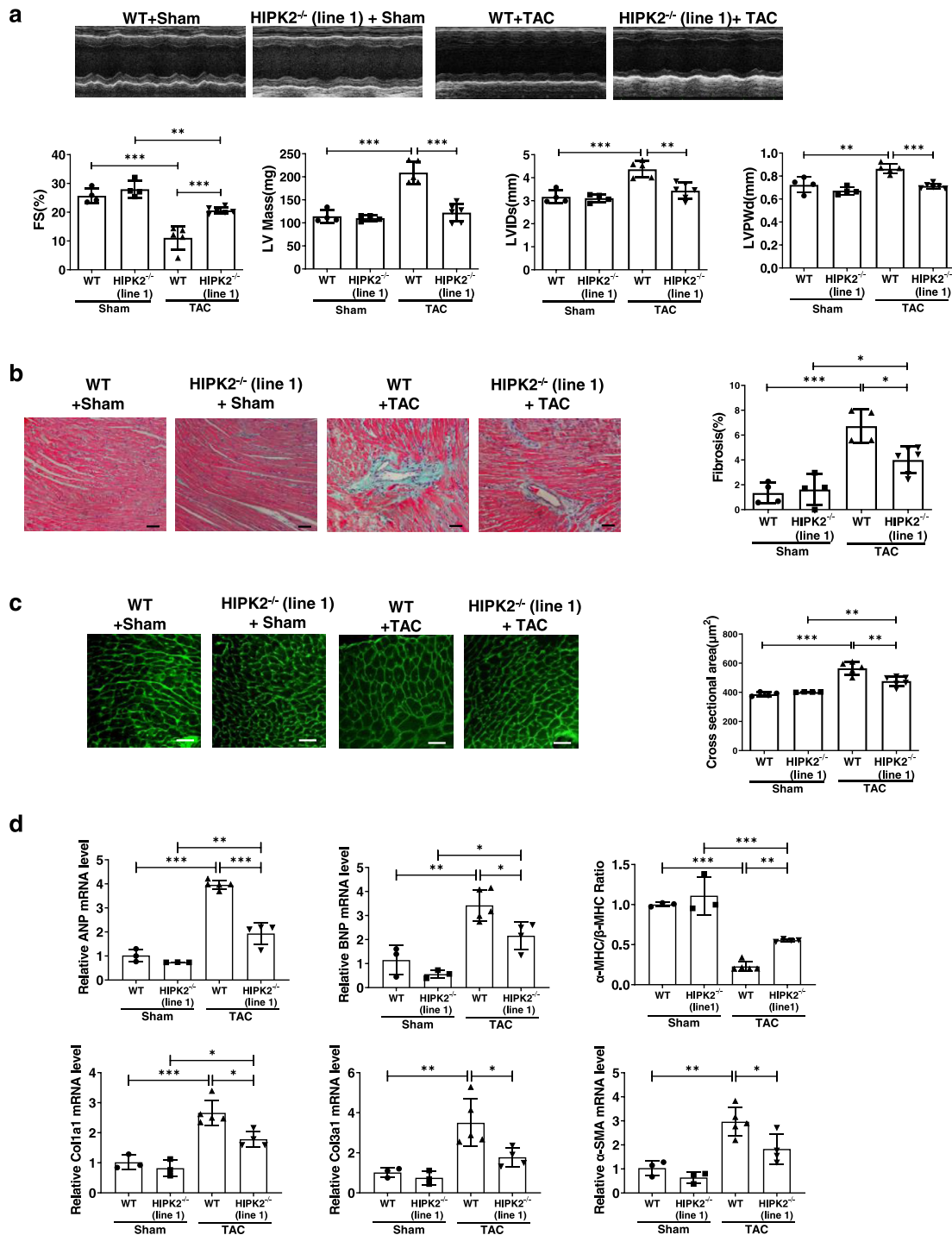
Figure 3. HIPK2 knock-out protects against cardiac dysfunction after TAC. (a) HIPK2$^{-/-}$ mice increased fractional shortening (FS) post-TAC, and reduced left ventricular (LV) mass, left ventricular systolic internal dimension (LVIDs) and left ventricular diastolic posterior wall (LVPWd) post-TAC (n=4:4:5:6); (b) HIPK2$^{-/-}$ mice reduced cardiac fibrosis post-TAC (n=4:4:4:6); (c) HIPK2$^{-/-}$ mice reduced cross sectional area of cardiomyocytes post-TAC (n=4:4:5:6); (d) HIPK2$^{-/-}$ mice decreased cardiac ANP, BNP, Col1a1, Col3a1, and α-SMA mRNA expression post-TAC, and increased ratio of α-MHC and β-MHC post-TAC (n=3:3:5:4). Scale bar: 50 μm in b and c. Significant differences were assessed by two-way ANOVA followed by Bonferroni's multiple comparisons test. *: $p<0.05$, **: $p<0.01$, ***: $p<0.001$ versus respective control.
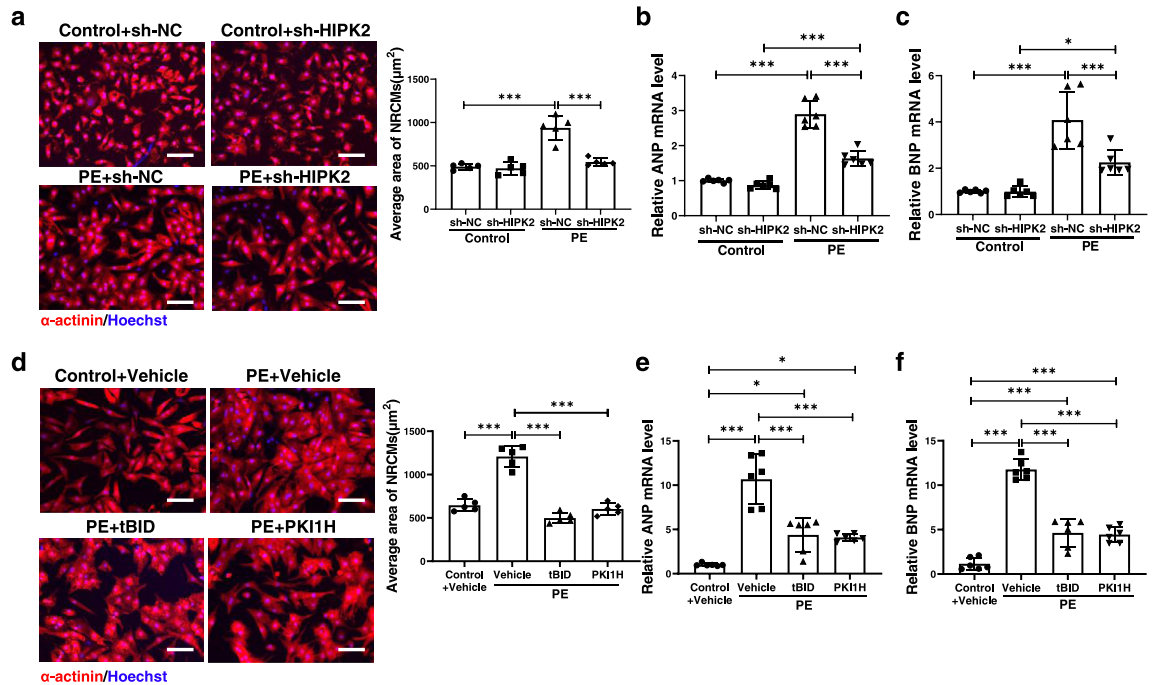
Figure 4. HIPK2 inhibition attenuates cardiomyocytes hypertrophy. (a-c) Lentiviruses expressing short-hairpin (sh) RNA against rat HIPK2 (shHIPK2) decreased cardiomyocytes areas (n=5), ANP and BNP mRNA expression (n=6) in NRCMs treated with PE. Immunofluorescent staining for α-actinin and Hoechst was used to label cardiomyocytes; (d-f) tBID and PKI1H decreased cardiomyocytes areas (n=5), ANP and BNP mRNA expression (n=6) in NRCMs treated with PE. Scale bar: 100 μm in a and d. Significant differences were assessed by two-way ANOVA followed by Bonferroni's multiple comparisons test. *: $p<0.05$, ***: $p<0.001$ versus respective control.

Affymetrix Gene Chip Array. A total of 21 genes showed marked changes in the heart of HIPK2$^{-/-}$ mice compared with the control mice (Figure 6a). We further validated these genes by qRT-PCRs (the CT value for Gsdma was below 35 and therefore excluded) and identified 10 genes that were significantly downregulated by HIPK2 knockout (Figure 6b). Next, we tested the expression of these 10 genes in the heart of TAC mice or sham mice and found 8 genes were significantly increased including Clec4d, Egr3, Cytokine receptor-like factor 1 (Crlf1), a disintegrin and metalloproteinase with thrombospondin motifs 4 (Adamts4), fibrillin-1 (Fbn1), heme oxygenase 1 (Hmox1), epiplakin 1 (Eppk1), neurexophilin and PC-esterase 5 (Nxpe5) (Figure 6c). Next, we determined these 8 genes' mRNA expression in the heart of I/R injury mice and found 6 genes were changed (Figure 6d). Consistent with these mRNA data, we found that EGR3, CLEC4D, CRLF1, ADAMTS4, FBN1 and HMOX1 protein abundance was decreased in the heart of HIPK2$^{-/-}$ mice (Supplemental Figure S15a). In addition, TAC increased EGR3, CLEC4D and CRLF1 protein abundance (Supplemental Figure S15b). As TGF-β did not affect EGR3, CLEC4D and CRLF1 in NRCFs (Supplemental Figure S16), and PE increased EGR3 and CLEC4D expression in NRCMs (Figure 6e), we hypothesized that EGR3 and CLEC4D

might be involved in HIPK2 inhibition-mediated cardiomyocytes hypertrophy regulation. EGR3 and CLEC4D protein expression levels were decreased by Lenti-shHIPK2 or HIPK2 inhibitors, and increased by Lenti-HIPK2 in NRCMs (Supplemental Figure S17). Furthermore, we found that EGR3 and CLEC4D overexpression could reverse the anti-hypertrophy effect of HIPK2 suppression in NRCMs treated with PE (Figure 6f-k). Collectively, EGR3 and CLEC4D mediate the protective effect of HIPK2 inhibition on cardiac hypertrophic growth.

HIPK2 has been reported to maintain basal cardiac function by activating phosphorylation of ERK1/2.[16] To clarify the role of ERK1/2 in our model, we firstly analyzed the phosphorylation of ERK1/2 by HIPK2 inhibition in cardiomyocytes and fibroblasts. HIPK2 inhibitors decreased the phosphorylation of ERK1/2 in heart including in control and TAC (Supplemental Figure S18). In NRCMs, HIPK2 overexpression could increase the phosphorylation of ERK1/2 while HIPK2 inhibition could decrease that (Supplemental Figure S19), while HIPK2 did not regulate that in NRCFs (Supplemental Figure S20). Besides, the phosphorylation of ERK1/2 was increased in PE-treated NRCMs (Supplemental Figure S21a). These data suggest that phosphorylation of ERK1/2 might be responsible for the effects of HIPK2 in cardiomyocytes but not in fibroblasts.
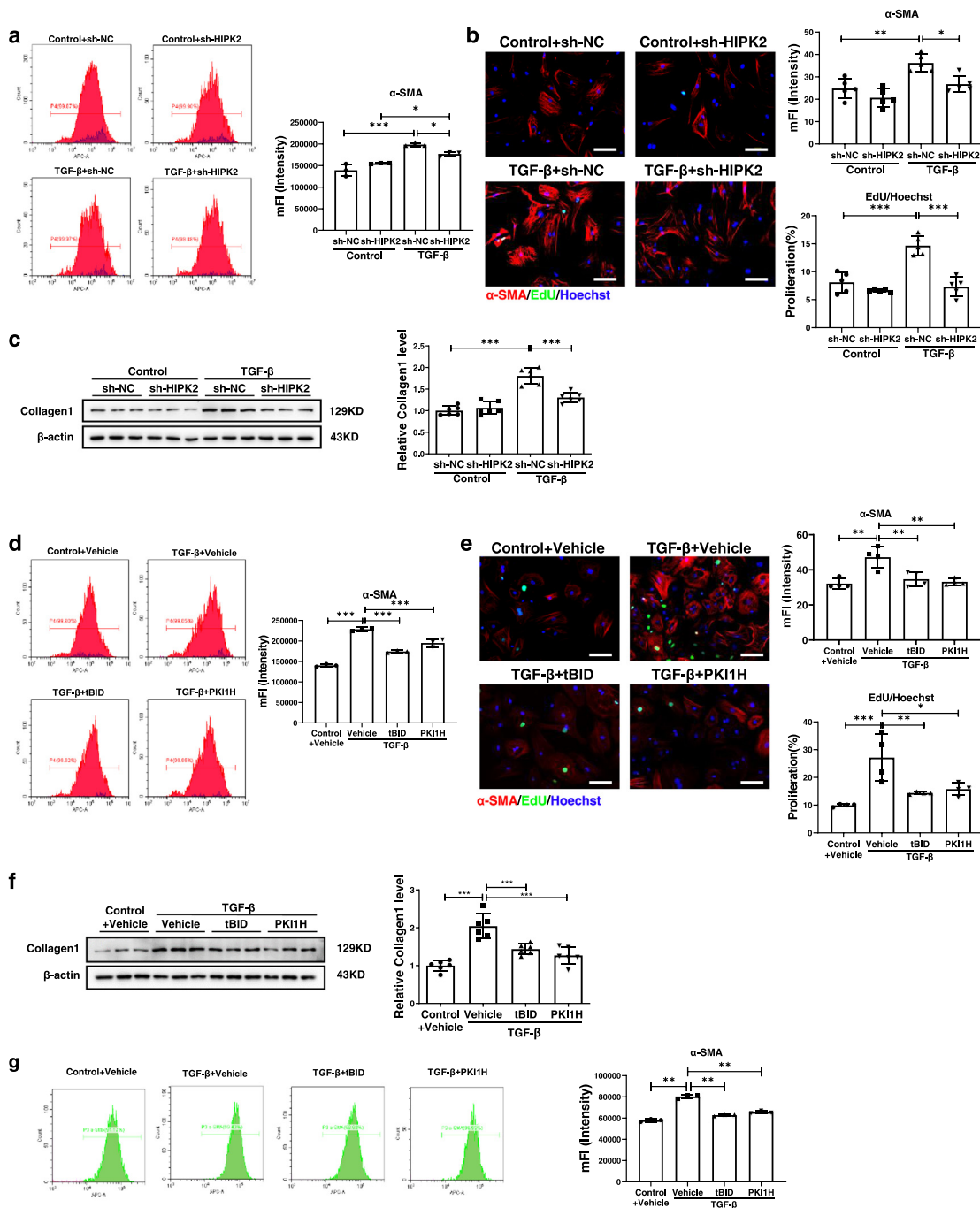
Figure 5. Inhibition of HIPK2 decreases cardiac fibroblasts proliferation and differentiation. (a-c) Lentiviruses of shHIPK2 decreased NRCFs proliferation and differentiation into myofibroblasts under TGF-β treatment as demonstrated by flow cytometry of α-SMA (*n*=3), immunofluorescent staining for α-SMA, EdU and Hoechst (*n*=5), and western blotting of Collagen1 (*n*=6); (d-f) tBID and PKI1H decreased NRCFs' proliferation and differentiation into myofibroblasts under TGF-β treatment as demonstrated by flow cytometry of α-SMA (*n*=3), immunofluorescent staining for α-SMA, EdU and Hoechst (*n*=4), and western blotting of Collagen1 (*n*=6); (g) tBID and PKI1H decreased RCFs' differentiation into myofibroblasts under TGF-β treatment as demonstrated by flow cytometry of α-SMA (*n*=3). Scale bar: 100 μm in b and e. Significant differences were assessed by two-way ANOVA followed by Bonferroni's multiple comparisons test. *: $p<0.05$, **: $p<0.01$, ***: $p<0.001$ versus respective control.
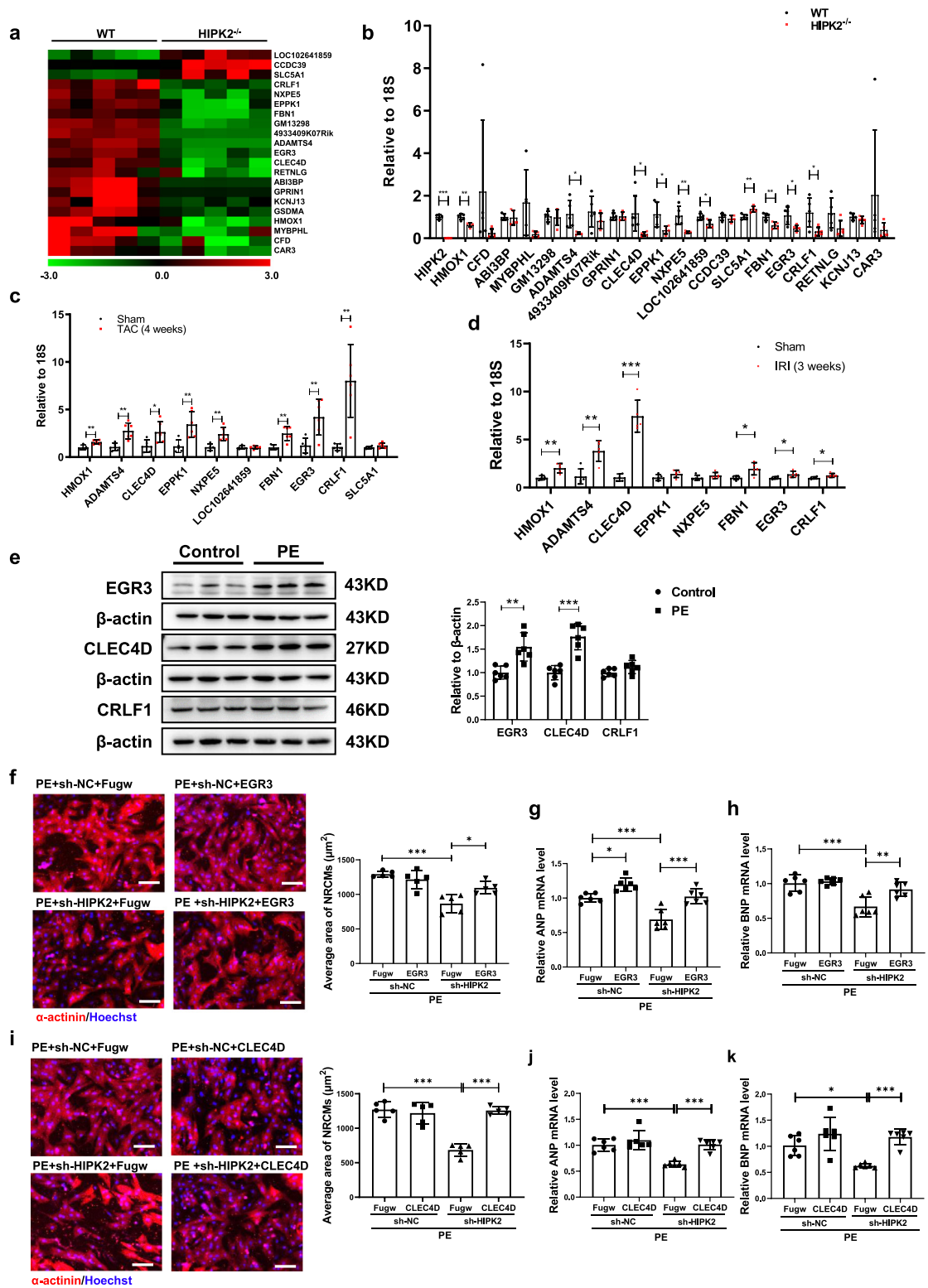
Figure 6. EGR3 and CLEC4D are identified as novel downstream of HIPK2 and their downregulation mediates the protection of HIPK2 inhibition in cardiomyocytes hypertrophy. (a) Affymetrix Gene Chip Array identified 21 genes as indicated markedly changed in the heart of HIPK2$^{-/-}$ mice compared with the control mice (n=5); (b) mRNA levels of 21 genes as indicated were

ERK1/2 activation could reverse the protection of HIPK2 suppression on NRCMs hypertrophy (Supplemental Figure S21b). ERK1/2 has been reported as an upstream regulator of EGR3 in mouse muscle.[32] Ceramide C6, an ERK1/2 activator increased EGR3, while PD98059, an ERK1/2 inhibitor decreased that in NRCMs (Supplemental Figure S22a-b). EGR3 overexpression could reverse the protective effects of ERK1/2 inhibition in PE-induced NRCMs hypertrophy (Supplemental Figure S22c). CLEC4D, as the other downstream regulator of HIPK2, was also found to be increased by Ceramide C6 and decreased by PD98059 (Supplemental Figure S22a-b). Moreover, CLEC4D overexpression could also reverse the protective effects of ERK1/2 inhibition in NRCMs hypertrophy induced by PE (Supplemental Figure S22d). To further investigate how ERK1/2 regulate EGR3 and CLEC4D, we determined its downstream CREB. We found that activation of ERK1/2 could increase the phosphorylation of CREB at serine 133 while inhibition of ERK1/2 could decrease that (Supplemental Figure S23). Moreover, knock-down of CREB decreased the expression of EGR3 and CLEC4D while overexpression of CREB increased them (Supplemental Figure S24). Furthermore, we found that HIPK2 inhibitors decreased the phosphorylation of ERK1/2 and CREB, and decreased EGR3 and CLEC4D in human cardiomyocyte cell line AC16 cells (Supplemental Figure S25). Taken together, these data suggest that inhibition of HIPK2 protects NRCMs hypertrophy through ERK1/2-CREB inhibition mediated EGR3 and CLEC4D downregulation.

Inhibition of phosphorylation of Smad3 mediates the suppression of fibroblast proliferation and differentiation by HIPK2 inhibition

Phosphorylation of Smad3 has been shown to be a target of HIPK2 in kidney fibrosis and is involved in cardiac dysfunction.[14,33,34] Very recently, the potential role of smad3 and HIPK2 in Angiotensin II induces cardiac fibrosis was reported.[35] However, whether inhibition of phosphorylation of Smad3 mediates the suppression of NRCFs proliferation and differentiation by HIPK2 inhibition is unclear. As expected, in the heart of control mice, HIPK2 inhibitors decreased phosphorylation of Smad3 at S423/425 and T179 (Figure 7a). Further, in

the heart of TAC, HIPK2 inhibitors could also decrease phosphorylation of Smad3 at S423/425 and T179 (Figure 7b). Besides, in HIPK2 knockout mice, the phosphorylation of Smad3 at S423/425 and T179 was decreased in the heart of TAC (Figure 7c). Meanwhile, the phosphorylation of Smad3 was decreased in NRCFs treated with HIPK2 inhibitors or lenti-shHIPK2, while increased in NRCFs treated with lenti-HIPK2 (Supplemental Figure S26). Overall, all above results suggest that Smad3 is a downstream target of HIPK2.

We next asked if inhibition of phosphorylation of Smad3 might be responsible for the suppression of NRCFs proliferation and differentiation by HIPK2 inhibition. Alantolactone, a Smad3 activator, rescued the anti-proliferative and anti-differentiative effects of HIPK2 suppression in NRCFs treated with TGF-β (Figure 7d-e and Supplemental Figure S27).

Taken together, inhibition of phosphorylation of Smad3 is required for the suppression effects of HIPK2 inhibition in NRCFs proliferation and differentiation.

AAV9 mediates knock-down of EGR3 or CLEC4D protects against pathological cardiac remodeling

To further investigate whether inhibition of EGR3 or CLEC4D could mimic the beneficial effects of HIPK2 suppression on cardiac dysfunction, we subjected mice to TAC surgery. AAV9 mediates knock-down of EGR3 in mice preserved cardiac function of TAC injury, as confirmed by increased FS, and decreased LV mass, LVIDs, and LVPWd (Figure 8a). Moreover, knock-down of EGR3 decreased cardiac fibrosis, cardiomyocyte cross sectional area, HW/BW, HW/TL, and promoted myocardial capillary (Figure 8b-d and Supplemental Figure S28). Besides, AAV9 mediates knock-down of CLEC4D in mice also achieved protective effects in TAC injury (Figure 8e-h, Supplemental Figure S29).

Collectively, AAV9 mediates knock-down of EGR3 or CLEC4D can protect against TAC induced pathological hypertrophy, suggesting potential novel therapeutics for pathological cardiac remodeling and heart failure.

Discussion

Heart failure is a common end-stage outcome of cardiovascular diseases with poor prognosis, which lacks of

---

analyzed in heart of control WT littermates and HIPK2$^{-/-}$ mice, and 10 genes mRNA levels were markedly changed in the heart of HIPK2$^{-/-}$ mice compared with the control mice (*n*=5); (c) mRNA levels of 10 genes as indicated were analyzed in heart of mice subjected to sham or TAC at 4 weeks after sham or TAC, and 8 genes mRNA levels were markedly changed in the heart of TAC mice compared with the sham mice (*n*=5:6); (d) mRNA levels of 8 genes as indicated were analyzed in heart of mice subjected to sham or I/R injury at 3 weeks after sham or I/R injury, and 6 genes mRNA levels were markedly changed in the heart of I/R injury mice compared with the sham mice (*n*=5); (e) PE increased EGR3 and CLEC4D protein levels in NRCMs (*n*=6); (f-h) Overexpression of EGR3 reversed the decreased cardiomyocytes areas (*n*=5), ANP and BNP mRNA expression (*n*=6) in NRCMs treated with lentiviruses of shHIPK2 in the presence of PE; (i-k) Overexpression of CLEC4D reversed the decreased cardiomyocytes areas (*n*=5), ANP and BNP mRNA expression (*n*=6) in NRCMs treated with lentiviruses of shHIPK2 in the presence of PE. Scale bar: 100 μm in f and i. Significant differences were assessed by two-tailed student t-test in b-e, or two-way ANOVA followed by Bonferroni's multiple comparisons test in f-k. *: *p*<0.05, **: *p*<0.01, ***: *p*<0.001 versus respective control.
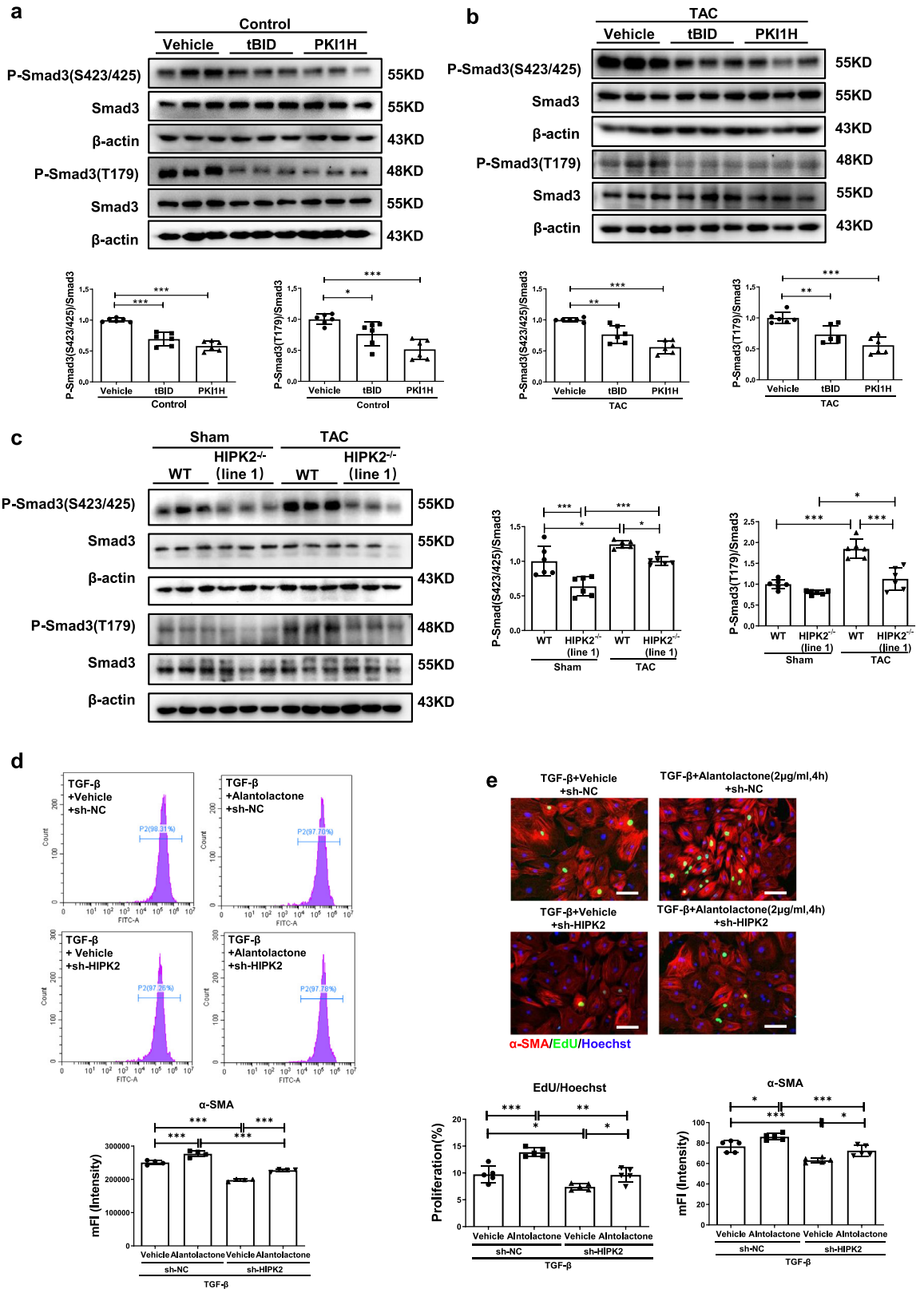
Figure 7. Phosphorylation of Smad3 is involved in the suppression of HIPK2 in cardiac fibroblasts proliferation and differentiation. (a) tBID and PKI1H decreased cardiac P-Smad3(S423/425) and P-Smad3(T179) in control mice (*n*=6); (b) tBID and PKI1H

treatable clinical intervention targets.[36] Therefore, it is of great significance to explore new approaches to prevent and treat heart failure. Here, we demonstrate that inhibition of HIPK2 protects against cardiac dysfunction induced by stress, supported by evidence from both pharmacological and genetic interventions. As summarized in Supplemental Figure S30, TAC up-regulates cardiac HIPK2. HIPK2 inhibition by inhibitors (tBID or PKI1H), or HIPK2$^{-/-}$ mice reduces hypertrophy through suppressing EGR3 and CLEC4D by inhibition of ERK1/2-CREB in cardiomyocytes. On the other hand, HIPK2 inhibition prevents cardiac fibroblasts proliferation and differentiation by suppressing the phosphorylation of Smad3. All these data suggest a distinct role of HIPK2 inhibition in cardiomyocytes and fibroblasts. Taken together, our findings suggest that blockage of HIPK2 could be a potential strategy for the prevention of pathological cardiac remodeling and heart failure.

HIPK2 inhibition has been reported to suppress neuronal differentiation, white adipose cell differentiation and erythroid differentiation.[9,11,37] Consistent with the impeding effect of HIPK2 on differentiation in other types of cells, we found that HIPK2 inhibition prevents cardiac fibroblast proliferation and differentiation. In addition, HIPK2 inhibition suppresses cardiac fibrosis, consistent with the anti-fibrosis effect of HIPK2 inhibition in kidney fibrosis.[13] On the other hand, HIPK2 has been reported to maintain basal cardiac function by activating phosphorylation of ERK1/2.[16] Our findings confirmed the previous findings that HIPK2$^{-/-}$ mice show no change in cardiac fibrosis and pathological hypertrophy compared with the control mice at 2 month old. However, we found that HIPK2$^{-/-}$ deficiency prevents cardiac dysfunction induced by TAC. We speculate that at baseline, heart function is normal and cannot be further improved. Thus, the protective effect of HIPK2 knockout can only be found under stressed conditions. To clarify the divergent results between Guo *et al.* and our work, we firstly analyzed the phosphorylation of ERK1/2 by HIPK2 inhibition in NRCMs and NRCFs. Consistent with their study, HIPK2 inhibitors decreased the phosphorylation of ERK1/2 in heart, as well as HIPK2 induced phosphorylation of ERK1/2 activation in NRCMs and vice versa. However, HIPK2 did not affect phosphorylation of ERK1/2 in NRCFs. It is known that ERK plays an important role during development as well as maintain physiological heart function, however, elevated ERK activity is detrimental during stress situations such as pathological

cardiac hypertrophy. In addition, cardiac-specific deletion of ERK1/2 generated by Nkx2.5-Cre or α-myosin heavy chain (α-MHC)-Cre shows cardiac dysfunction and heart failure.[38] In contrast, left ventricular cardiac tissue samples of patients with heart failure showed phosphorylation of ERK1/2 activation and ERK1/2 positively led to fibrosis, hypertrophy and cardiac dysfunction.[39] According to the above findings, ERK1/2 may play different roles in cardiomyocytes and cardiac fibroblasts. Secondly, we and Guo *et al.* utilized different construction strategies for HIPK2$^{-/-}$ mice. Our two founders of C57BL/6 HIPK2$^{-/-}$ mice were generated by embryo injection of guide RNA targeting the second exon of the mouse *HIPK2* gene, which introduces frameshift mutations of 56bp and 40bp deletions, respectively. Guo *et al.* used homologous recombination with the targeting construct deleting exon 3 (the first coding exon) to generate HIPK2 null mice in 129 and B6 mixed background.[40] The same mice strain as ours showed reduced blood glucose and high-fat diet induced weight gain.[11] These data suggest that HIPK2 inhibition is beneficial. As the expression of cardiac HIPK2 in advanced stage ischemic heart failure was shown to be decreased,[16] thus, this strategies of inhibiting HIPK2 might have a limitation for its use under this condition. Besides, as HIPK2 deletion causes cardiac dysfunction during aging (at 5 month),[16] this indicates that long term suppression of HIPK might be very detrimental. Nevertheless, in this study, we proved the protection of HIPK2 inhibition on pathological cardiac remodeling not only by HIPK2$^{-/-}$ deletion in mice, but also by pharmacological HIPK2 inhibition. Additionally, we have revealed the role of HIPK2 inhibition in cardio-protection through cardiomyocytes and cardiac fibroblasts. The two chemicals inhibitors we used are specific for HIPK2.[19,20] For the doses of tBID and PKI1H, we detected the downstream of HIPK2 to make sure the doses we selected are working.

We used Affymetrix Gene Chip Array to screen HIPK2 targets and identified that EGR3 and CLEC4D may participate in the effect of HIPK2 inhibition on cardiac function. As a zinc-finger transcription factor, EGR3 was reported to be involved in angiogenesis and nervous system development.[41,42] In consistent with HIPK2 inhibition effect on cardiac function, EGR3 expression is activated after chronic myocardial infarction.[43] In addition, cardiac fibrosis significantly upregulates EGR3, which suggests the involvement of EGR3 in cardiac fibrosis.[44,45] Although previous results show that a 4-hour TGF-β treatment induces EGR3

decreased cardiac P-Smad3(S423/425) and P-Smad3(T179) post-TAC (*n*=6); (c) HIPK2-/- mice decreased cardiac P-Smad3(S423/425) and P-Smad3(T179) protein levels in TAC (*n*=6); (d-e) Smad3 activator (Alantolactone) reversed the reduction of NRCFs proliferation and differentiation into myofibroblasts by lentiviruses of shHIPK2 decreased under TGF-β treatment as demonstrated by flow cytometry of α-SMA (*n*=4), immunofluorescent staining for α-SMA, EdU and Hoechst (*n*=5). Scale bar: 100 μm in e. Significant differences were assessed by one-way ANOVA followed by Bonferroni's post hoc test in a-b, or two-way ANOVA followed by Bonferroni's multiple comparisons test in c-e. *: $p<0.05$, **: $p<0.01$, ***: $p<0.001$ versus respective control.
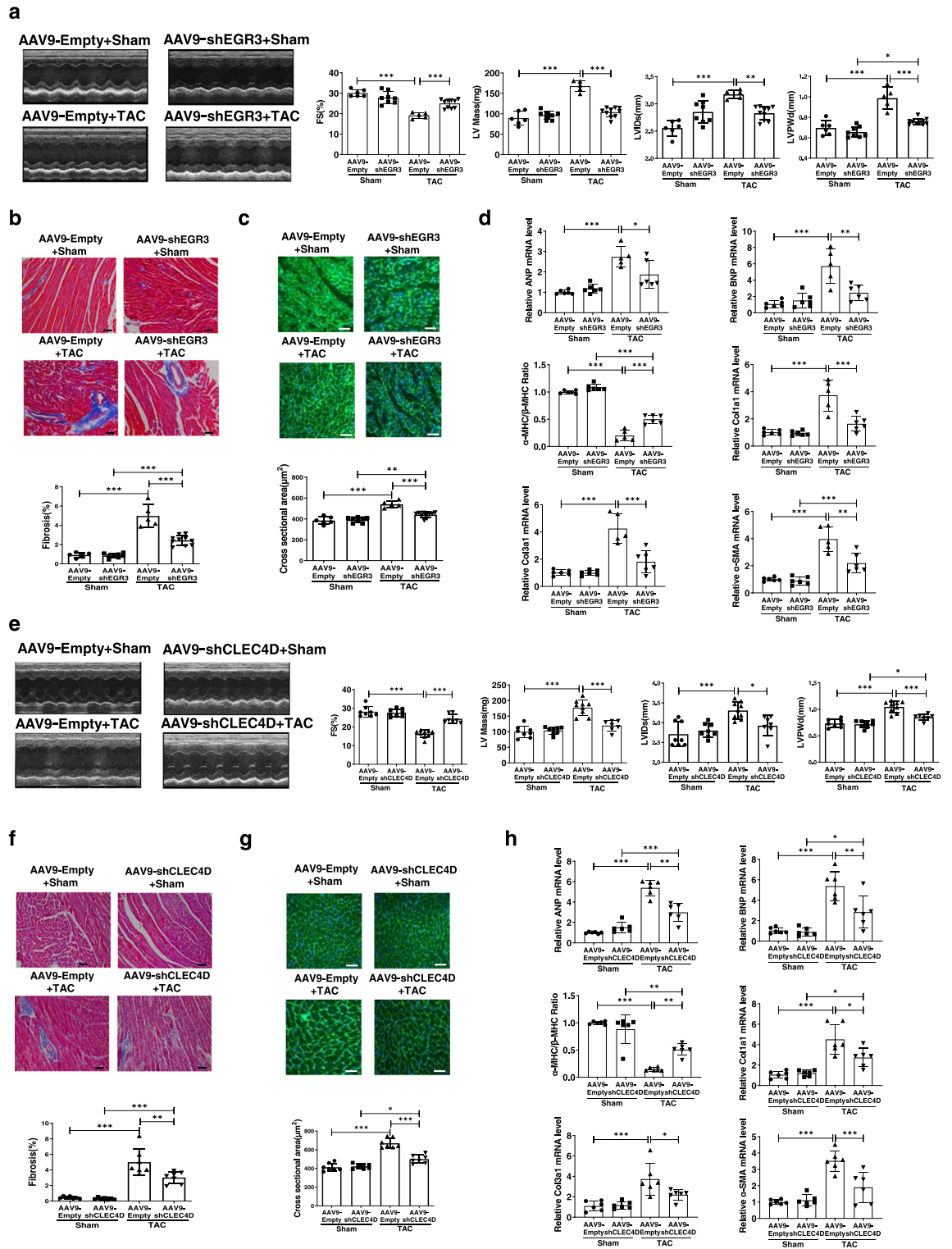
Figure 8. Inhibition of EGR3 or CLEC4D protects against TAC. (a) Inhibition of EGR3 increased fractional shortening (FS) after TAC, and reduced left ventricular (LV) mass, left ventricular systolic internal dimension (LVIDs) and left ventricular diastolic posterior wall (LVPWd) after TAC (n=6:8:5:10); (b) Inhibition of EGR3 reduced cardiac fibrosis after TAC (n=6:8:5:10); (c) Inhibition of EGR3 reduced cross sectional area of cardiomyocytes after TAC (n=6:8:5:10); (d) Inhibition of EGR3 decreased cardiac ANP, BNP, Col1a1, Col3a1,

expression in adult skin fibroblasts[46] our data show no change of EGR3 expression in NRCFs under TGF-β treatment. It might be due to the different types of cell lines and the different duration of TGF-β treatment. The role of CLEC4D in heart is unclear. Its family member, CLEC4E, a necrotic cell sensor, was reported to promote cholesterol efflux and to drive inflammation induced by factors released by necrotic cells. Knockout CLEC4E in macrophage reduces lipid accumulation, endoplasmic reticulum stress, and inflammation in arterial lesions and relieves atherosclerosis.[47] TGF-β/Smad3 pathway was reported to be involved in HIPK2-mitigated kidney fibrosis.[14] Smad3 signaling was activated in the infarcted myocardium.[48] In addition, cardiomyocyte-specific Smad3 KO mice attenuates remodeling and dysfunction after infarction.[49] Of note, a recent study reported that HIPK2 knockdown could attenuate Angiotensin II induced cardiac fibrosis in *vitro*, potentially by inhibition of Smad3.[35] However, whether inhibition of phosphorylation of Smad3 mediates the suppression of cardiac fibroblasts proliferation and differentiation by HIPK2 inhibition is unclear. Here, we show the involvement of Smad3 phosphorylation in HIPK2 inhibition-mediated cardioprotective effect. Consistently, cardiac phosphorylation of Smad3 is decreased by HIPK2 inhibition in cardiac tissues and in NRCFs. Furthermore, activation of Smad3 reverses the ability of HIPK2 inhibition to prevent an increase in proliferation and differentiation of NRCFs. Together, our data suggest that EGR3 and CLEC4D in cardiomyocytes, and phosphorylation of Smad3 in fibroblasts, are involved in HIPK2 inhibition-mediated cardiac protection.

The novelty of our work was as follows. Firstly, we report that HIPK2 inhibition is sufficient to reduce cardiac remodeling and improve heart failure by a dual cellular mechanism including both cardiomyocytes and cardiac fibroblasts. Secondly, we identify CLEC4D and EGR3 as two downstream targets of HIPK2, mediating its effects in cardiomyocytes hypertrophy. Thirdly, we show the function of CLEC4D in heart and found that AAV9 mediates knock-down of CLEC4D protects against TAC induced cardiac remodeling and heart failure.

Several limitations of the present study should be highlighted. Firstly, mice with cardiomyocyte-specific and cardiac fibroblast-specific knockout of HIPK2 should be added. Through these two kinds of mice, we will not only further confirm the roles of HIPK2 inhibition in cardio-protection, but also understand the contribution of HIPK2 inhibition in cardiomyocytes and fibroblasts. Secondly, detailed mechanisms underlying HIPK2-mediated control of EGR3 and CLEC4D expression remain to be further explored, especially for how ERK1/2-CREB regulates EGR3 and CLEC4D. Thirdly, since HIPK2 has a physiological role in maintaining the normal development and function of the heart, it is unclear whether chronic inhibition of HIPK2 would lead to deleterious effects or not. Fourthly, although we analyzed almost most commonly used parameters in TAC model, it would be interesting to measure transaortic pressure gradients to better standardise or characterise the model in the future. Fifthly, although the concentrations of PE (100 μM) in NRCMs and 100 μM ISO in combination with PE in hESC-CMs have been used in the literature,[25−27,29] they might be suprapatophysiological concentrations.

In summary, we have demonstrated that inhibiting HIPK2 protects against pathological cardiac remodeling induced by TAC through reducing EGR3 and CLEC4D in cardiomyocytes, and reducing the phosphorylation of Smad3 in fibroblasts. Our findings provide new insights into the roles of HIPK2 inhibition in cardiomyocytes and cardiac fibroblasts, respectively, and suggest that inhibition of HIPK2 will be a potential target for therapeutic interventions in heart failure.

Data sharing statement
The data for this study are available by contacting the corresponding author upon reasonable request.

Declaration of interests
The authors have declared that no conflict of interest exists.

and α-SMA mRNA expression post-TAC, and increased ratio of α-MHC and β-MHC post-TAC (n=6:6:5:6); (e) Inhibition of CLEC4D increased fractional shortening (FS) after TAC, and reduced left ventricular (LV) mass, left ventricular systolic internal dimension (LVIDs) and left ventricular diastolic posterior wall (LVPWd) after TAC (n=8:8:9:7); (f) Inhibition of CLEC4D reduced cardiac fibrosis after TAC (n=7:7:7:7); (g) Inhibition of CLEC4D reduced cross sectional area of cardiomyocytes after TAC (n=7:7:7:7); (h) Inhibition of CLEC4D decreased cardiac ANP, BNP, Col1a1, Col3a1, and α-SMA mRNA expression post-TAC, and increased ratio of α-MHC and β-MHC post-TAC (n=6). Scale bar: 50 μm in b, c, f, and g. Significant differences were assessed by two-way ANOV followed by Bonferroni's multiple comparisons test. *: $p < 0.05$, **: $p < 0.01$, ***: $p < 0.001$ versus respective control.

Supplementary materials

Supplementary material associated with this article can be found in the online version at doi:10.1016/j.ebiom.2022.104274.

References

1 Granger CB, McMurray JJ, Yusuf S, et al. Effects of candesartan in patients with chronic heart failure and reduced left-ventricular systolic function intolerant to angiotensin-converting-enzyme inhibitors: the CHARM-Alternative trial. *Lancet*. 2003;362(9386):772–776.

2 Bei Y, Wang L, Ding R, et al. Animal exercise studies in cardiovascular research: Current knowledge and optimal design-A position paper of the committee on cardiac rehabilitation, Chinese medical doctors' association. *J Sport Health Sci*. 2021;10(6):660–674.

3 Chen S, Zhang Y, Lighthouse JK, et al. A novel role of cyclic nucleotide phosphodiesterase 10A in pathological cardiac remodeling and dysfunction. *Circulation*. 2020;141(3):217–233.

4 McLaughlin S, McNeill B, Podrebarac J, et al. Injectable human recombinant collagen matrices limit adverse remodeling and improve cardiac function after myocardial infarction. *Nat Commun*. 2019;10(1):4866.

5 Xiao J, Rosenzweig A. Exercise and cardiovascular protection: update and future. *J Sport Health Sci*. 2021;10(6):607–608.

6 Conte A, Pierantoni GM. Update on the regulation of HIPK1, HIPK2 and HIPK3 protein kinases by microRNAs. *Microrna*. 2018;7(3):178–186.

7 Kim YH, Choi CY, Lee SJ, Conti MA, Kim Y. Homeodomain-interacting protein kinases, a novel family of co-repressors for homeodomain transcription factors. *J Biol Chem*. 1998;273(40):25875–25879.

8 Wook Choi D, Yong Choi C. HIPK2 modification code for cell death and survival. *Mol Cell Oncol*. 2014;1(2):e955999.

9 Ciarapica R, Methot L, Tang Y, et al. Prolyl isomerase Pin1 and protein kinase HIPK2 cooperate to promote cortical neurogenesis by suppressing Groucho/TLE:Hes1-mediated inhibition of neuronal differentiation. *Cell Death Differ*. 2014;21(2):321–332.

10 de la Vega L, Hornung J, Kremmer E, Milanovic M, Schmitz ML. Homeodomain-interacting protein kinase 2-dependent repression of myogenic differentiation is relieved by its caspase-mediated cleavage. *Nucleic Acids Res*. 2013;41(11):5731–5745.

11 Sjolund J, Pelorosso FG, Quigley DA, DelRosario R, Balmain A. Identification of Hipk2 as an essential regulator of white fat development. *Proc Natl Acad Sci U S A*. 2014;111(20):7373–7378.

12 Chalazonitis A, Tang AA, Shang Y, et al. Homeodomain interacting protein kinase 2 regulates postnatal development of enteric dopaminergic neurons and glia via BMP signaling. *J Neurosci*. 2011;31(39):13746–13757.

13 Jin Y, Ratnam K, Chuang PY, et al. A systems approach identifies HIPK2 as a key regulator of kidney fibrosis. *Nat Med*. 2012;18(4):580–588.

14 Liu R, Das B, Xiao W, et al. A novel inhibitor of homeodomain interacting protein kinase 2 mitigates kidney fibrosis through inhibition of the TGF-beta1/Smad3 pathway. *J Am Soc Nephrol*. 2017;28(7):2133–2143.

15 Wei G, Ku S, Ma GK, et al. HIPK2 represses beta-catenin-mediated transcription, epidermal stem cell expansion, and skin tumorigenesis. *Proc Natl Acad Sci U S A.*. 2007;104(32):13040–13045.

16 Guo Y, Sui JY, Kim K, et al. Cardiomyocyte homeodomain-interacting protein kinase 2 maintains basal cardiac function via extracellular signal-regulated kinase signaling. *Circulation*. 2019;140(22):1820–1833.

17 Liu X, Xiao J, Zhu H, et al. miR-222 is necessary for exercise-induced cardiac growth and protects against pathological cardiac remodeling. *Cell Metab*. 2015;21(4):584–595.

18 Zhou Q, Deng J, Yao J, et al. Exercise downregulates HIPK2 and HIPK2 inhibition protects against myocardial infarction. *EBioMedicine*. 2021;74:103713.

19 Cozza G, Zanin S, Determann R, Ruzzene M, Kunick C, Pinna LA. Synthesis and properties of a selective inhibitor of homeodomain-interacting protein kinase 2 (HIPK2). *PLoS One*. 2014;9(2):e89176.

20 Miduturu CV, Deng X, Kwiatkowski N, et al. High-throughput kinase profiling: a more efficient approach toward the discovery of new kinase inhibitors. *Chem Biol*. 2011;18(7):868–879.

21 Piccoli MT, Gupta SK, Viereck J, et al. Inhibition of the cardiac fibroblast-enriched lncRNA Meg3 prevents cardiac fibrosis and diastolic dysfunction. *Circ Res*. 2017;121(5):575–583.

22 Bei Y, Pan LL, Zhou Q, et al. Cathelicidin-related antimicrobial peptide protects against myocardial ischemia/reperfusion injury. *BMC Med*. 2019;17(1):42.

23 Gao R, Wang L, Bei Y, et al. Long noncoding RNA cardiac physiological hypertrophy-associated regulator induces cardiac physiological hypertrophy and promotes functional recovery after myocardial ischemia-reperfusion injury. *Circulation*. 2021;144(4):303–317.

24 Ritterhoff J, Young S, Villet O, et al. Metabolic remodeling promotes cardiac hypertrophy by directing glucose to aspartate biosynthesis. *Circ Res*. 2020;126(2):182–196.

25 Gao L, Huang K, Jiang DS, et al. Novel role for caspase-activated DNase in the regulation of pathological cardiac hypertrophy. *Hypertension*. 2015;65(4):871–881.

26 Jiang DS, Liu Y, Zhou H, et al. Interferon regulatory factor 7 functions as a novel negative regulator of pathological cardiac hypertrophy. *Hypertension*. 2014;63(4):713–722.

27 Yang Y, Del Re DP, Nakano N, et al. miR-206 mediates yap-induced cardiac hypertrophy and survival. *Circ Res*. 2015;117(10):891–904.

28 Wang H, Maimaitiaili R, Yao J, et al. Percutaneous intracoronary delivery of plasma extracellular vesicles protects the myocardium against ischemia-reperfusion injury in Canis. *Hypertension*. 2021;78(5):1541–1554.

29 Viereck J, Kumarswamy R, Foinquinos A, et al. Long noncoding RNA Chast promotes cardiac remodeling. *Sci Transl Med*. 2016;8(326):326ra22.

30 Li J, Chan MC, Yu Y, et al. miR-29b contributes to multiple types of muscle atrophy. *Nat Commun*. 2017;8:15201.

31 Luo X, Yin J, Dwyer D, et al. Chamber-enriched gene expression profiles in failing human hearts with reduced ejection fraction. *Sci Rep*. 2021;11(1):11839.

32 Herndon CA, Ankenbruck N, Fromm L. The Erk MAP kinase pathway is activated at muscle spindles and is required for induction of the muscle spindle-specific gene Egr3 by neuregulin1. *J Neurosci Res*. 2014;92(2):174–184.

33 Gao Y, Zhang YM, Qian LJ, Chu M, Hong J, Xu D. ANO1 inhibits cardiac fibrosis after myocardial infraction via TGF-beta/smad3 pathway. *Sci Rep*. 2017;7(1):2355.

34 Yan Z, Shen D, Liao J, et al. Hypoxia suppresses TGF-B1-induced cardiac myocyte myofibroblast transformation by inhibiting Smad2/3 and Rhoa signaling pathways. *Cell Physiol Biochem*. 2018;45(1):250–257.

35 Xu F, Mao B, Li Y, Zhao Y. Knockdown of HIPK2 attenuates angiotensin II-induced cardiac fibrosis in cardiac fibroblasts. *J Cardiovasc Pharmacol*. 2022;80(1):125–131.

36 Bass-Stringer S, Tai CMK, McMullen JR. IGF1-PI3K-induced physiological cardiac hypertrophy: Implications for new heart failure therapies, biomarkers, and predicting cardiotoxicity. *J Sport Health Sci*. 2021;10(6):637–647.

37 Hattangadi SM, Burke KA, Lodish HF. Homeodomain-interacting protein kinase 2 plays an important role in normal terminal erythroid differentiation. *Blood*. 2010;115(23):4853–4861.

38 Kehat I, Davis J, Tiburcy M, et al. Extracellular signal-regulated kinases 1 and 2 regulate the balance between eccentric and concentric cardiac growth. *Circ Res*. 2011;108(2):176–183.

39 Thum T, Gross C, Fiedler J, et al. MicroRNA-21 contributes to myocardial disease by stimulating MAP kinase signalling in fibroblasts. *Nature*. 2008;456(7224):980–984.

40 Wiggins AK, Wei G, Doxakis E, et al. Interaction of Brn3a and HIPK2 mediates transcriptional repression of sensory neuron survival. *J Cell Biol*. 2004;167(2):257–267.

41 Eldredge LC, Gao XM, Quach DH, et al. Abnormal sympathetic nervous system development and physiological dysautonomia in Egr3-deficient mice. *Development*. 2008;135(17):2949–2957.

42 Liu D, Evans I, Britton G, Zachary I. The zinc-finger transcription factor, early growth response 3, mediates VEGF-induced angiogenesis. *Oncogene*. 2008;27(21):2989–2998.

43 Saddic LA, Howard-Quijano K, Kipke J, et al. Progression of myocardial ischemia leads to unique changes in immediate-early gene expression in the spinal cord dorsal horn. *Am J Physiol Heart Circ Physiol*. 2018;315(6):H1592–HH601.

44 Teng L, Huang Y, Guo J, et al. Cardiac fibroblast miR-27a may function as an endogenous anti-fibrotic by negatively regulating early growth response protein 3 (EGR3). *J Cell Mol Med*. 2021;25(1):73–83.

45 Udoko AN, Johnson CA, Dykan A, et al. Early regulation of profibrotic genes in primary human cardiac myocytes by Trypanosoma cruzi. *PLoS Negl Trop Dis*. 2016;10(1):e0003747.

46 Fang F, Shangguan AJ, Kelly K, et al. Early growth response 3 (Egr-3) is induced by transforming growth factor-beta and regulates fibrogenic responses. *Am J Pathol*. 2013;183(4):1197–1208.

47 Clement M, Basatemur G, Masters L, et al. Necrotic cell sensor Clec4e promotes a proatherogenic macrophage phenotype through activation of the unfolded protein response. *Circulation*. 2016;134(14):1039–1051.

48 Bujak M, Ren G, Kweon HJ, et al. Essential role of Smad3 in infarct healing and in the pathogenesis of cardiac remodeling. *Circulation*. 2007;116(19):2127–2138.

49 Kong P, Shinde AV, Su Y, et al. Opposing actions of fibroblast and cardiomyocyte smad3 signaling in the infarcted myocardium. *Circulation*. 2018;137(7):707–724.